Singlets in lattice gauge theories coupled to matter fields in multiple representations

Nuno Brito, Ed Bennett, Deog Ki Hong, Jong-Wan Lee, C.-J. David Lin, Biagio Lucini, Maurizio Piai, Davide Vadacchino and Fabian Zierler

July 28, 2026

The 43rd International Symposium on Lattice Field Theory, University of Maryland, College Park, United States of America

UNIVERSITY OF PLYMOUTH

Introduction

Sympletic gauge theories

- QCD's $SU(3)_c \longrightarrow Sp(4)_c$;
- Two fermion species:
  1. $Q^a \longrightarrow U^{ab} Q^b$;
  2. $\Psi^{ab} \longrightarrow U^{ac} U^{bd} \Psi^{cd}$;
- Different symmetry-breaking patterns $\implies$ model building possibilities:

Sympletic gauge theories

- QCD's $SU(3)_c \longrightarrow Sp(4)_c$;
- Two fermion species:
  1. $Q^a \longrightarrow U^{ab}Q^b$;
  2. $\Psi^{ab} \longrightarrow U^{ac}U^{bd}\Psi^{cd}$;
- Different symmetry-breaking patterns $\implies$ model building possibilities:
  1. Composite Higgs Model;
  2. Top partial compositeness;
  3. Composite Dark Model;

Global flavour symmetry

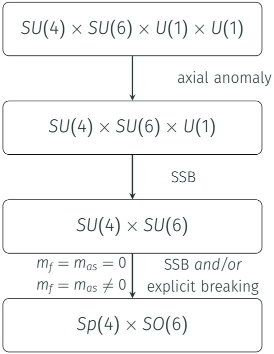

This work: $N_f = 2, N_{as} = 3$ **flavour singlets, (σ and η') + glueball operators.**

TELOS Collaboration Review: @ https://arxiv.org/pdf/2304.01070

Setup

Meson Correlators

- Connected and disconnected contributions for each fermion type:

$$C^{\Gamma}_{\mathrm{f-f}}(x,y) = \pm$$

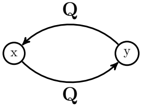

$$+ N_{\mathrm{f}}$$

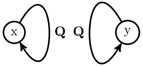

,

$$C^{\Gamma}_{\mathrm{as-as}}(x,y) = \pm$$

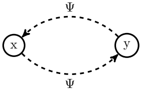

$$+ N_{\mathrm{as}}$$

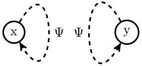

,

$$C^{\Gamma}_{\mathrm{f-as}}(x,y) = +\sqrt{N_{\mathrm{as}} N_{\mathrm{f}}}$$

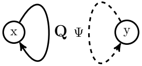

,

Meson Correlators

- Connected and disconnected contributions for each fermion type:

$C^{\Gamma}_{\mathrm{f-f}}(x, y) = \pm$ 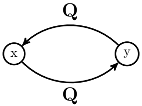

$+ N_{\mathrm{f}}$ 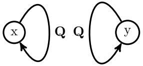

,

$C^{\Gamma}_{\mathrm{as-as}}(x, y) = \pm$ 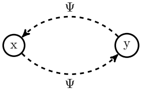

$+ N_{\mathrm{as}}$ 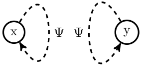

,

$C^{\Gamma}_{\mathrm{f-as}}(x, y) = +\sqrt{N_{\mathrm{as}} N_{\mathrm{f}}}$ 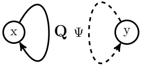

,

- Connected contributions: single-source inversion of $D^{(\mathrm{R})}(x; y)$;
- Disconnected contributions: spin-diluted stochastic sources with $Z_2 \times Z_2$ noise;

- Connected and disconnected contributions for each fermion type:

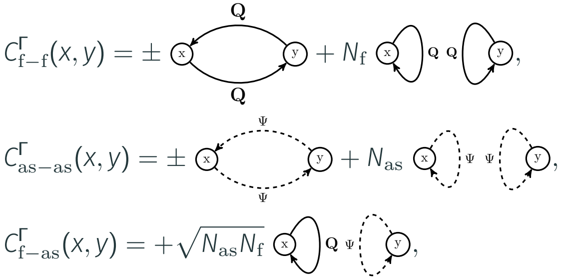

- Connected contributions: single-source inversion of $D^{(\mathrm{R})}(x; y)$;
- Disconnected contributions: spin-diluted stochastic sources with $Z_2 \times Z_2$ noise;
- Basis with local and APE + Wuppertal smeared operators.

TELOS Collaboration - Physical Review D 110, no. 7 (2024): 074504.

Glueball Correlators

- Built from spatial Wilson loops;
- Projected into irreducible representations $\mathcal{R}$ of the octahedral group O_h:

$$O_G^{\mathcal{R}}[U](x) = \sum_{g \in O_h} c_g^{\mathcal{R}} \, \mathrm{Tr}\, g(U)$$

  for prototype loop shape U.
- Parity defined via:

$$O_G^{\mathcal{R}^{P=\pm}} = O_G^{\mathcal{R}} \pm \mathcal{P}(O_G^{\mathcal{R}})$$

- Pseudo-reality of $Sp(4)$ representations $\implies C = +$;

Glueball Correlators

- Built from spatial Wilson loops;
- Projected into irreducible representations $\mathcal{R}$ of the octahedral group O_h:

$$O_G^{\mathcal{R}}[U](x) = \sum_{g \in O_h} c_g^{\mathcal{R}} \, \mathrm{Tr}\, g(U)$$

  for prototype loop shape U.
- Parity defined via:

$$O_G^{\mathcal{R}^{P=\pm}} = O_G^{\mathcal{R}} \pm \mathcal{P}(O_G^{\mathcal{R}})$$

- Pseudo-reality of $Sp(4)$ representations $\implies C = +$;
- Improved APE-smearing + Blocking.

Generalized Eigenvalue Problem (GEVP)

- Correlation Matrix:

$$C_{ij} = \begin{pmatrix} C_{\mathrm{G-G}} & C_{\mathrm{G-f}} & C_{\mathrm{G-as}} \\ C_{\mathrm{f-G}} & C_{\mathrm{f-f}} & C_{\mathrm{f-as}} \\ C_{\mathrm{as-G}} & C_{\mathrm{as-f}} & C_{\mathrm{as-as}} \end{pmatrix}$$

- *Partial-pruning* procedure to mitigate smearing degeneracies:

$$C_{\mathrm{op-op}}(t_0) = U^{\dagger}_{\mathrm{op}}(t_0)\, \Sigma_{\mathrm{op-op}}\, V_{\mathrm{op}}(t_0)$$

- Generalized Eigenvalue Problem:

$$C(t_0)v(t_0,t_1) = \lambda(t_0,t_1)C(t_1)v(t_0,t_1), \quad D_i(t) \equiv v_i^T(t_0,t_1)C(t)v_i(t_0,t_1);$$

- Bayesian model averaging based on AIC criterion in fitting time ranges:

$$\mathrm{AIC}[m] = \left(\chi^{(m)}\right)^2 + 2n^{(m)}_{\mathrm{param}} - n^{(m)}_{\mathrm{data}}, \quad \omega^{(m)} \propto e^{-\frac{1}{2}\mathrm{AIC}[m]}$$

Urrea-Niño, Juan Andrés, et al. Physical Review D 114.1 (2026): 014509.
Jay, William I., and Ethan T. Neil. Physical Review D 103, no. 11 (2021): 114502
See also Li, Qu-Zhi, Chuan Liu, Liuming Liu, Peng Sun, Jia-Jun Wu, Zhiguang Xiao, and Han-Qing Zheng. arXiv:2603.16266.

Ensembles

- Two ensembles studied:

Label	β	am_0^{as}	am_0^{f}	N_t	N_s	N_{conf}	$\langle P \rangle$	w_0/a
M3	6.5	-1.01	-0.71	96	20	4507	0.585156(13)	2.5170(40)
M4	6.5	-1.01	-0.70	64	20	5683	0.584228(12)	2.3557(31)

- Wilson gauge and fermion action;
- Heavy quark masses;
- Software: GRID (generation) and HiRep (measurements).

HiRep: Del Debbio, Luigi, Agostino Patella, and Claudio Pica. Physical Review D 81.9 (2010): 094503.
GRID: Boyle, Peter, Azusa Yamaguchi, Guido Cossu, and Antonin Portelli. arXiv:1512.03487 (2015).

Measurements - Spectroscopy

Results: Pseudoscalar

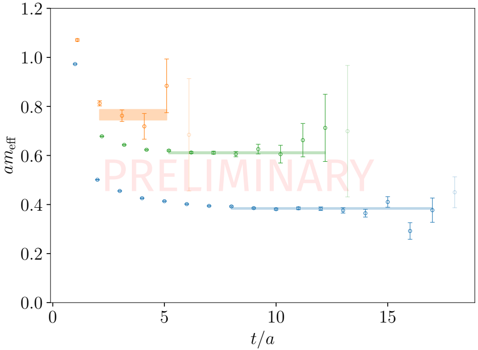

Figure 1: Effective mass in the pseudoscalar channel for the M3 ensemble (data-points) and fit result (shaded regions) from the model averaging procedure (vertical span - energy and uncertainty, horizontal span - times considered in model averaging procedure).

Results: Pseudoscalar

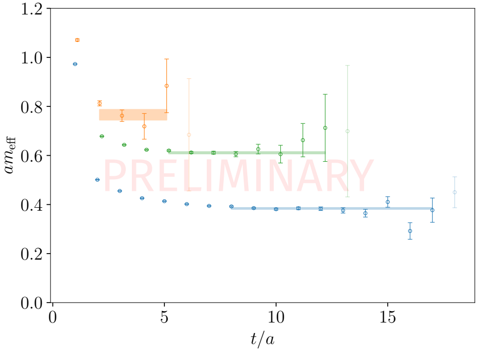

Figure 1: Effective mass in the pseudoscalar channel for the M3 ensemble (data-points) and fit result (shaded regions) from the model averaging procedure (vertical span - energy and uncertainty, horizontal span - times considered in model averaging procedure).

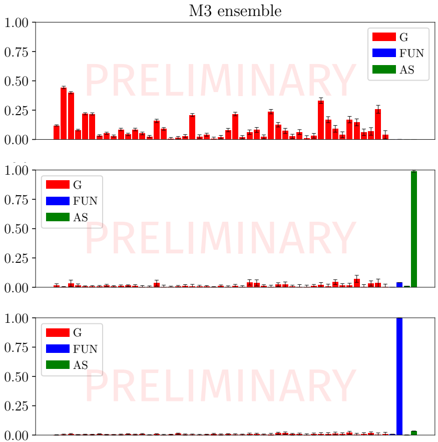

Figure 2: Coefficients of GEVP eigenvectors $v(t_0, t_1)$.

Results: Scalar

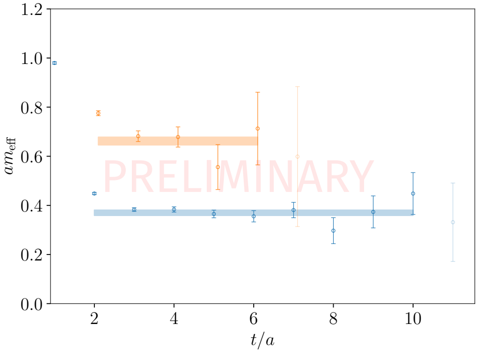

Figure 3: Effective mass in the scalar channel for the M3 ensemble (data-points) and fit result (shaded regions) from the model averaging procedure (vertical span - energy and uncertainty, horizontal span - times considered in model averaging procedure).

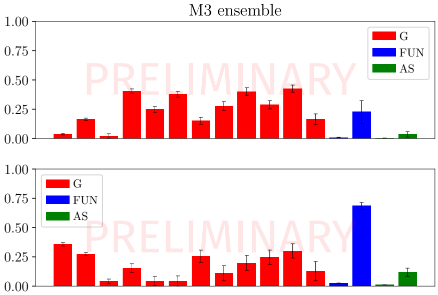

Figure 4: Coefficients of GEVP eigenvectors $v(t_0, t_1)$.

Results: Basis restriction

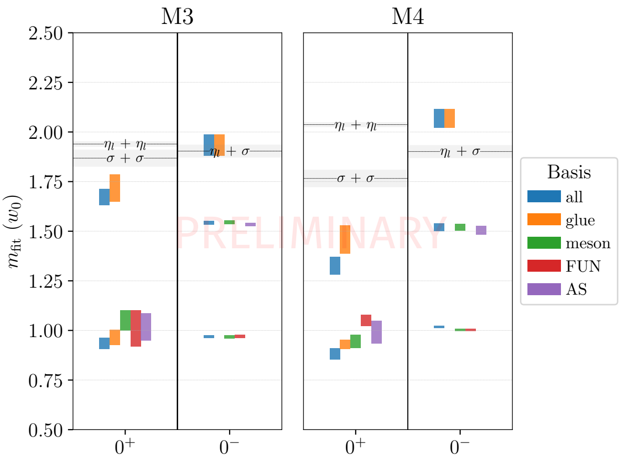

Figure 5: Energy levels obtained with different operator basis.

- Variational approach shows improvement in the scalar channel as operator basis is extended;
- If new signal in pseudoscalar channel is a state, it is on threshold on M3, unstable on M4;
- Glueball operators work nicely in the scalar channel.

Full Spectra

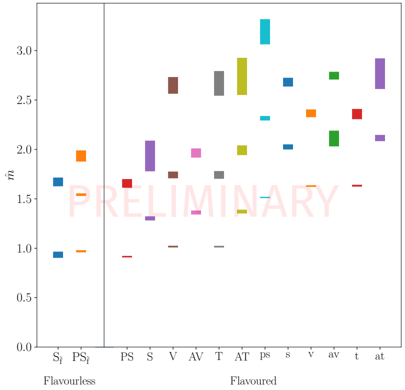

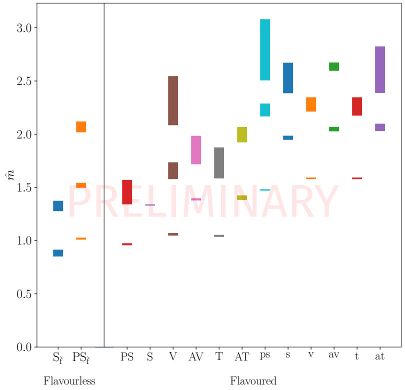

Figure 6: The flavoured meson spectrum and flavour singlet spectrum for the M3 ensemble (left) and M4 ensemble (right) in units of the Wilson flow scale. The vertical black line separates the flavour singlet spectrum (left) studied in this work from the flavoured meson spectrum (right).

TELOS Collaboration - Physical Review D 112, no. 7 (2025): 074515.

Measurements - Mixing Angles

Mixing Angles: $\eta'_l - \eta'_h$ angle

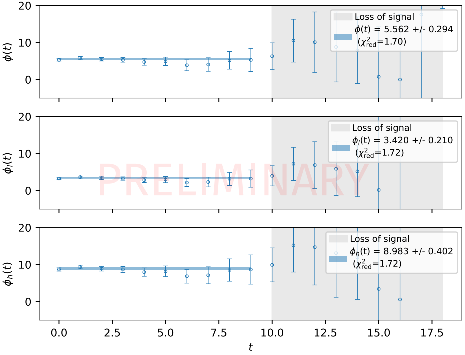

Figure 7: $\eta'_l - \eta'_h$ mixing angle in the M3 ensemble. Tested using a single angle parametrization ϕ (top panel) or two-angle parametrization $\phi_l - \phi_h$ (middle and bottom panel).

- Eigenstates as linear combination of *flavour-states*:

$$\begin{pmatrix} |\eta'_l\rangle \\ |\eta'_h\rangle \end{pmatrix} = \begin{pmatrix} \cos(\phi_l) & \sin(\phi_l) \\ -\sin(\phi_h) & \cos(\phi_h) \end{pmatrix} \cdot \begin{pmatrix} |\eta'_{\mathrm{fun}}\rangle \\ |\eta'_{\mathrm{as}}\rangle \end{pmatrix}$$

- Small angles - heavy fermion masses $\implies$ $\eta'_l - \eta'_h$ mixing effects surpressed;
- $\phi_l \neq \phi_h \implies$ two-angles required to parametrize.

TELOS Collaboration - Physical Review D 110, no. 7 (2024): 074504.

Mixing Angles: Meson-Glueball angle

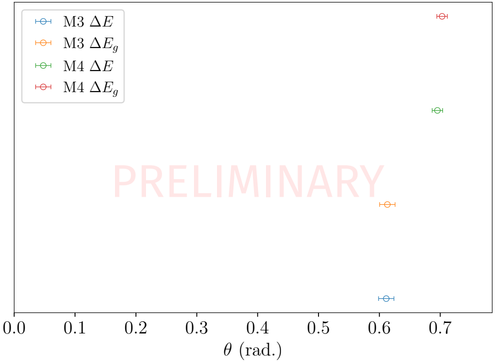

Figure 8: *Meson-Glueball* angle for both ensembles extracted from energies obtained when considering the full operator basis and restricted versions of it.

- Linear combination:

$$\begin{pmatrix} |Q\rangle \\ |G\rangle \end{pmatrix} = \begin{pmatrix} \cos(\theta) & \sin(\theta) \\ \sin(\varphi) & \cos(\varphi) \end{pmatrix} \cdot \begin{pmatrix} |\psi_0\rangle \\ |\psi_1\rangle \end{pmatrix}$$

- $E_g - E_Q = (E_1 - E_0)\ \cos 2\theta$;
- Attempt to approximate $\Delta E = E_1 - E_0$ with glue basis $\Delta E_g = E_1^{(g)} - E_0^{(g)}$;
- Large mixing angle, but different across ensembles;
- Meson-glueball mixing (?).

See also: L. C. Gui, W. Sun, Y. Chen, M. Gong, G. Li and Z. Liu, 'Scalar glueball-$s\bar{s}$ mixing in one flavor lattice QCD,'

Summary & Outlook

Summary & Outlook

Takeaways:

- Scalar and pseudoscalar flavour singlet spectroscopy with matter fields in multiple representations;
- Two ensembles with heavy fermion masses;
- Glueball-sourced signal on threshold;
- Hints of meson-glue mixing in scalar channel;

Outlook:

- Treatment of systematic uncertainties;
- Multi-particle operators in GEVP;
- Improved action;
- Distillation;
- Renormalization procedure.

End

Backup Slides

TELOS References

Past work (pure gauge):

- Glueballs: 1712.04220, 2010.15781
- Fund and AS flavoured mesons: 1912.06505
- Topology: 2205.09254, 2205.09364
- Large-N: 2010.15781, 2312.08465

Dynamical studies:

- $N_f = 2$ flavoured mesons: 1911.00437
- $N_f = 2$ singlets (f_0 and η'): 1911.00437
- $n_{as} = 3$ flavoured mesons: 2210.08154
- $N_f = 2, n_{as} = 3$ mesons from spectral densities: 2405.01388
- $N_f = 2, n_{as} = 3$ singlets (η'): 2405.05765

$Sp(2N)$ theories

- Sp(4) gauge theory;
- $N_f = 2$ fundamental fermions, $n_{as} = 3$ anti-symmetric fermions;
- Continuum Lagrangian:

$$\mathcal{L} = -\frac{1}{2}\mathrm{Tr} V_{\mu\nu}V^{\mu\nu} + \sum_{J=1}^{2}\left(i\,\overline{Q^J}_a\gamma^\mu\left(D_\mu Q^J\right)^a\right) - m^{(f)}\sum_{J=1}^{2}\overline{Q^J}_a Q^{J\,a} +$$

$$+\sum_{j=1}^{3}\left(i\,\overline{\Psi^j}_{ab}\gamma^\mu\left(D_\mu \Psi^j\right)^{ab}\right) - m^{(as)}\sum_{j=1}^{3}\overline{\Psi^j}_{ab}\Psi^{j\,ab}\,;$$

- $SU(4)\times SU(6) \xrightarrow[\text{sym. break}]{\text{explicit}} Sp(4)\times SO(6)$;
- $SU(4)/Sp(4)$: 5 pNGBs - (4 SM Higgs doublet, 1 extra);
- $SU(6)/SO(6)$: 20 pNGBs - *chimera baryons* mix with top quark.

TELOS Collaboration @ https://arxiv.org/pdf/2304.01070

Lattice Action

- Wilson gauge action:

$$S_g = \beta \sum_x \sum_{\mu<\nu} \left(1 - \frac{1}{2N} \mathrm{Re}\ \mathrm{Tr}\left(U_\mu(x) U_\nu(x+\hat{\mu}) U_\mu^\dagger(x+\hat{\nu}) U_\nu^\dagger(x)\right)\right)$$

- Wilson fermions:

$$S_f = a^4 \sum_{l=1}^{N_{\mathrm{f}}} \sum_{x,y} \overline{Q}^l(x) D^{(\mathrm{f})}(x,y) Q^l(y) + a^4 \sum_{k=1}^{N_{\mathrm{as}}} \sum_{x,y} \overline{\Psi}^k(x) D^{(\mathrm{as})}(x,y) \Psi^k(y)$$

- Different bare quark masses in $D^{(\mathrm{f})}(x,y)$ and $D^{(\mathrm{as})}(x,y)$.

Ensembles

- Two ensembles studied:

Label	β	am_0^{as}	am_0^{f}	N_t	N_s	N_{conf}	$\langle P \rangle$	w_0/a
M3	6.5	-1.01	-0.71	96	20	4507	0.585156(13)	2.5170(40)
M4	6.5	-1.01	-0.70	64	20	5683	0.584228(12)	2.3557(31)

- Wilson gauge and fermion action;
- Moderate-Heavy quark bare quark masses;
- Software: GRID (generation) and HiRep (measurements);

HiRep: Del Debbio, Luigi, Agostino Patella, and Claudio Pica. Physical Review D 81.9 (2010): 094503.
GRID: Boyle, Peter, Azusa Yamaguchi, Guido Cossu, and Antonin Portelli. arXiv:1512.03487 (2015).

Wilson Flow

$$\mathcal{W}(t)|_{t=w_0^2} = 0.2815, \quad \mathcal{W}(t) \equiv \frac{d}{d\ln(t)} \left\{ t^2 \langle E(t) \rangle \right\},$$

with

$$E(t,x) = -\frac{1}{2}\,\mathrm{Tr}\, G_{\mu\nu}(t,x) G^{\mu\nu}(t,x).$$

$E(x,t)$ written in terms of either four-leaf clover plaquette or simple plaquette action.

What is what?

Table 1: Interpolating operators $\mathcal{O}_M$ built with Dirac fermions of types (f) and (as). Colour and spinor indices are implicit and summed over, and flavor combinations are denoted generically. More details can be found in Ref. [?]. We also show the J^P quantum numbers, the corresponding QCD meson sourced by the operator with analogous quantum numbers, and the irreducible representation of the unbroken global $Sp(4) \times SO(6)$ symmetry groups.

Label M	Interpolating operator $\mathcal{O}_M$	Mesons in $N_f = 2$ QCD	J^P	$Sp(4)$	$SO(6)$
PS	$\overline{Q^I}\gamma_5 Q^J$	π	0^-	5	1
S	$\overline{Q^I}Q^J$	a_0	0^+	5	1
V	$\overline{Q^I}\gamma_\mu Q^J$	ρ, ρ'	1^-	10	1
T	$\overline{Q^I}\sigma_{\mu\nu} Q^J$	ρ, ρ'	1^-	10	1
AV	$\overline{Q^I}\gamma_5\gamma_\mu Q^J$	a_1	1^+	5	1
AT	$\overline{Q^I}\gamma_5\sigma_{\mu\nu} Q^J$	b_1	1^+	10	1
ps	$\overline{\Psi^k}\gamma_5 \Psi^j$	π	0^-	1	$20'$
s	$\overline{\Psi^k}\Psi^j$	a_0	0^+	1	$20'$
v	$\overline{\Psi^k}\gamma_\mu \Psi^j$	ρ, ρ'	1^-	1	15
t	$\overline{\Psi^k}\sigma_{\mu\nu} \Psi^j$	ρ, ρ'	1^-	1	15
av	$\overline{\Psi^k}\gamma_5\gamma_\mu \Psi^j$	a_1	1^+	1	$20'$
at	$\overline{\Psi^k}\gamma_5\sigma_{\mu\nu} \Psi^j$	b_1	1^+	1	15

Smearing Parameters

Table 2: Details on Wuppertal and APE smearing used on the mesonic operators across the considered ensembles.

Ensemble	Operator Species	N_{APE}	α_{APE}	α_{staple}	$N_{\mathrm{Wuppertal\ levels}}$	Step	ϵ_R	n_{src}
M3	Fundamental	50	0.4	0.4	5	50	0.3	100
	Antisymmetric				4	60		64
M4	Fundamental				11	20		32
	Antisymmetric				11	20		32

Table 3: Details on APE smearing and Blocked for the glueball operators across the considered ensembles.

Ensemble	Operator Species	N_{APE}	α_{APE}	α_{staple}	α_{diag}	N_{blocking}	N_{cooling}
M3	Glueball	4	1	2.4	0.16	4	5
M4							

Operator Summary

- Glueball basis:
  - 32 Prototype loop shapes;
  - 5 levels of Improved APE smear + Blocking;
  - Projection to $A_1^+ \to 160$ glueball operators;
  - Projection to $A_1^- \to 100$ glueball operators;
- Meson basis:
  - Wuppertal Smearing levels dependent on ensemble and representation:
  - Ensemble M3: 5 Fundamental, 4 Anti-symmetric;
  - Ensemble M4: 11 Fundamental, 11 Anti-symmetric;
  - Number of stochastic sources also dependent on ensemble and representation;
- Zero-momentum projected operators.

Results: Pseudoscalar - M4

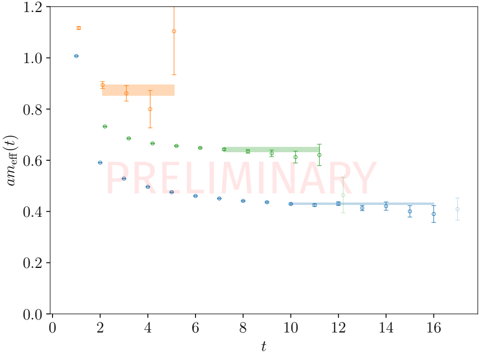

Figure 9: Effective mass in the pseudoscalar channel for the M4 ensemble (data-points) and fit result (shaded regions) from the model averaging procedure (vertical span - energy and uncertainty, horizontal span - times considered in model averaging procedure).

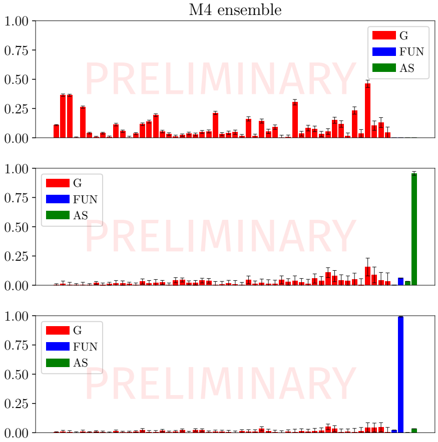

Figure 10: Coefficients of GEVP eigenvectors $v(t_0, t_1)$.

Results: Scalar - M4

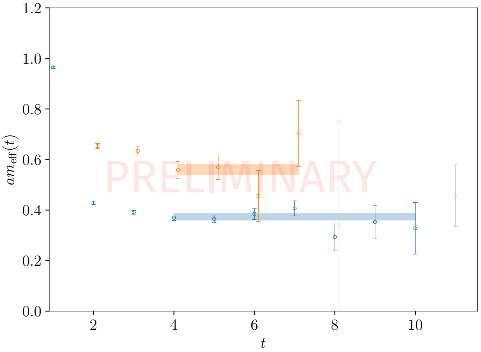

Figure 11: Effective mass in the scalar channel for the M4 ensemble (data-points) and fit result (shaded regions) from the model averaging procedure (vertical span - energy and uncertainty, horizontal span - times considered in model averaging procedure).

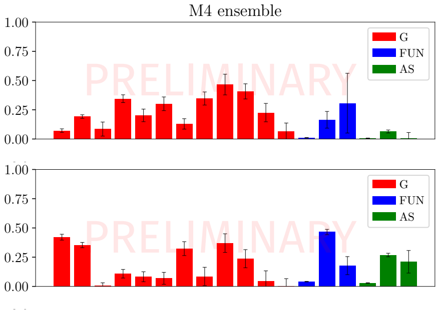

Figure 12: Coefficients of GEVP eigenvectors $v(t_0, t_1)$.

Why Model Averaging? (M3 - Pseudoscalar Groundstate)

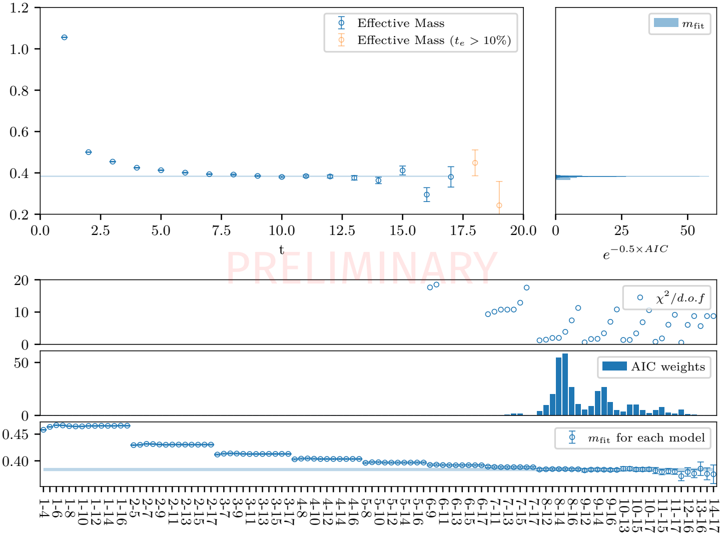

Why Model Averaging? (M3 - Scalar Groundstate)

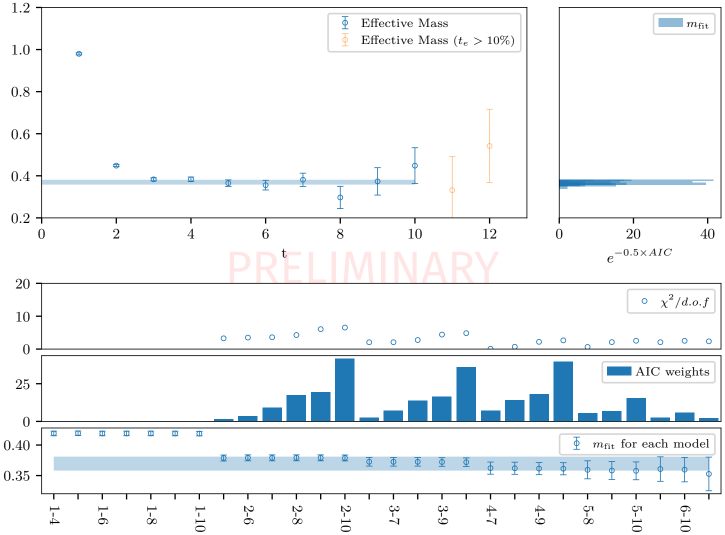

Effective mass choices

Log $am_{\text{eff}}(t)$:

$$am_{\text{eff}}(t) = \log\left(\frac{D(t)}{D(t+1)}\right)$$

Arccosh $am_{\text{eff}}(t)$:

$$am_{\text{eff}}(t) = \operatorname{arccosh}\left(\frac{D(t+a) - D(t-a)}{2D(t)}\right)$$

Effective mass choice (M3)

Arccosh Meff:

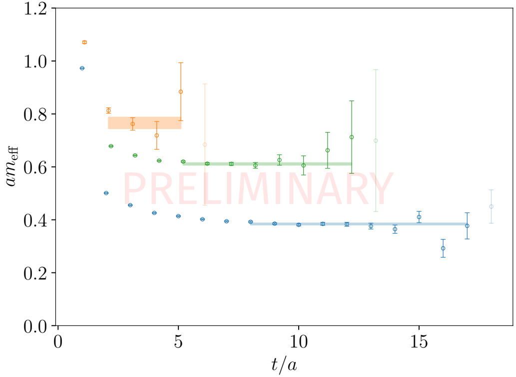

Log Meff:

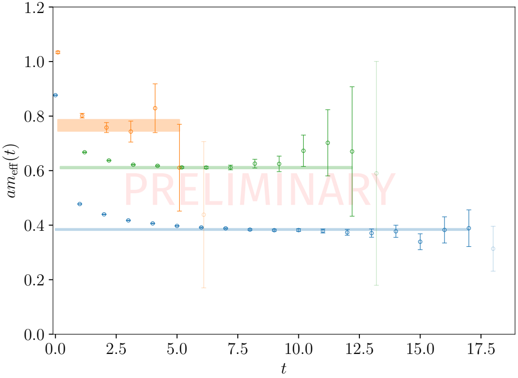

Effective mass choice (M4)

Arccosh Meff:

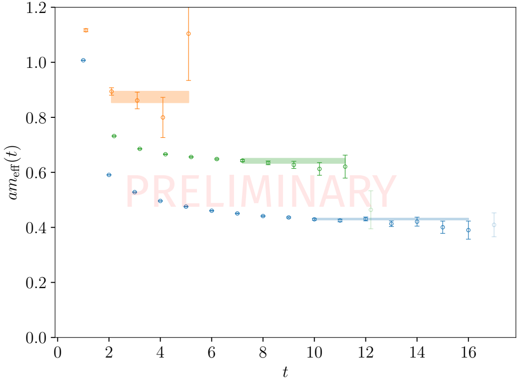

Log Meff:

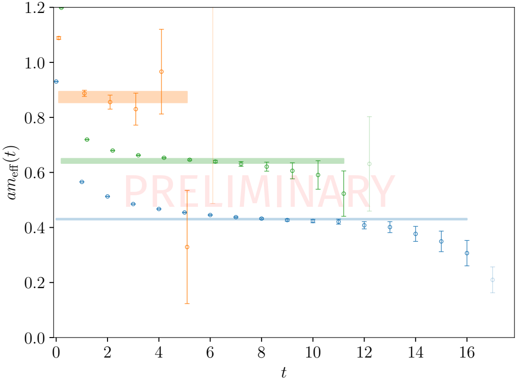

Mixing Angles: $\eta'_l - \eta'_h$ angle

- Analogous to $\eta - \eta'$ mixing in QCD:

$$\begin{pmatrix} |\eta'_l\rangle \\ |\eta'_h\rangle \end{pmatrix} = \begin{pmatrix} \langle\Omega|O_{\rm fun}|\eta'_l\rangle & \langle\Omega|O_{\rm as}|\eta'_l\rangle \\ \langle\Omega|O_{\rm fun}|\eta'_h\rangle & \langle\Omega|O_{\rm as}|\eta'_h\rangle \end{pmatrix} \cdot \begin{pmatrix} |\eta'_{\rm fun}\rangle \\ |\eta'_{\rm as}\rangle \end{pmatrix}$$

- Parametrize into either one or two angles:

$$\begin{pmatrix} |\eta'_l\rangle \\ |\eta'_h\rangle \end{pmatrix} = \begin{pmatrix} \cos(\phi_l) & \sin(\phi_l) \\ -\sin(\phi_h) & \cos(\phi_h) \end{pmatrix} \cdot \begin{pmatrix} |\eta'_{\rm fun}\rangle \\ |\eta'_{\rm as}\rangle \end{pmatrix}$$

- Only local operators (2×2 GEVP, with $t_0 = 5$);

TELOS Collaboration - Physical Review D 110, no. 7 (2024): 074504.

M3 Pseudoscalar Decoupling

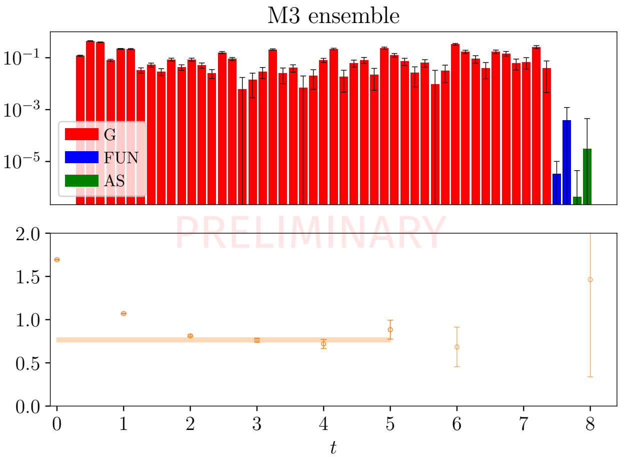

Figure 13: Upper pane - Overlaps for glueball-sourced signal on pseudoscalar channel in the M3 ensemble. Lower pane - Corresponding effective mass (data-points) and result from model averaging procedure (shaded rectangles).

Mixing Angles: $\eta'_l - \eta'_h$ angle

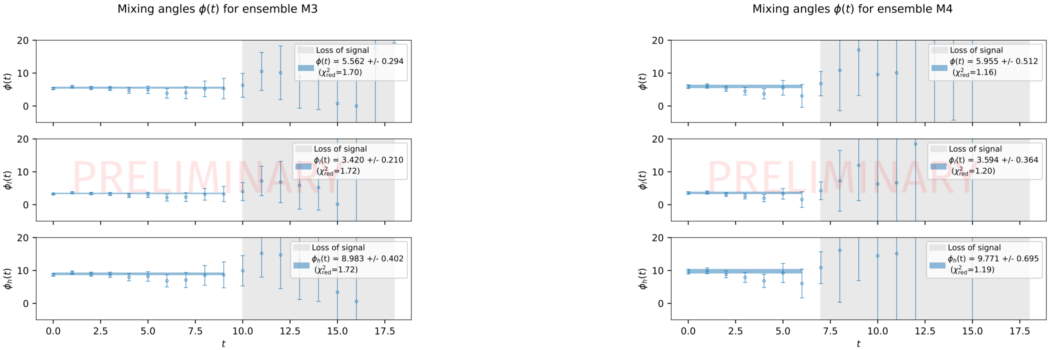

Figure 14: $\eta'_l - \eta'_h$ mixing angle in the M3 (left) and M4 (right) ensembles. Tested using a single angle parametrization ϕ (top panel) or two-angle parametrization $\phi_l - \phi_h$ (middle and bottom panel).

Mixing Angles: Meson-Glueball angle

- Parametrize linear combination:

$$\begin{pmatrix} |\psi_Q\rangle \\ |\psi_g\rangle \end{pmatrix} = \begin{pmatrix} \cos(\theta) & \sin(\theta) \\ \sin(\varphi) & \cos(\varphi) \end{pmatrix} \cdot \begin{pmatrix} |\psi_0\rangle \\ |\psi_1\rangle \end{pmatrix}$$

- Operators sourcing ψ_Q, ψ_g commute, so:

$$\langle \psi_Q | \psi_g \rangle = 0 \implies \cos(\theta - \varphi) = 0$$

- Angle obtained from relation:

$$E_g - E_Q = (E_1 - E_0)\ \cos 2\theta.$$